Weak interaction rates and shape coexistence for the $Z = N + 2$ isotopes ^{70}Kr and ^{74}Sr

A. Petrovici[*] and O. Andrei

National Institute for Physics and Nuclear Engineering - Horia Hulubei, R-077125 Bucharest, Romania
(Received 17 August 2015; revised manuscript received 18 November 2015; published 10 December 2015)

The weak interaction rates for the $Z = N + 2$ isotopes ^{70}Kr and ^{74}Sr dominated by shape coexistence are self-consistently investigated within the beyond-mean-field *complex* excited Vampir variational model using an effective interaction obtained from a G matrix based on the charge-dependent Bonn CD potential. Results are presented on β-decay properties under terrestrial conditions as well as the contribution of the thermally populated low-lying excited states of ^{70}Kr and ^{74}Sr in the x-ray burst astrophysical environment on the effective half-lives.

I. INTRODUCTION

Proton-rich nuclei in the $A \sim 70$ mass region are intensively investigated both theoretically and experimentally since their properties are relevant for the astrophysical rapid proton capture (rp) process and could bring insights into fundamental symmetries and interactions. These nuclei manifest exotic nuclear structure and dynamics generated by the interplay between shape coexistence and mixing, competing like-nucleon and neutron-proton $T = 1$ and $T = 0$ pairing correlations, and isospin-symmetry-breaking interactions. Of particular importance could be the β-decay properties of the low-lying excited states of proton-rich nuclei situated on the rp-process path whose thermal population may influence their effective half-lives at the high temperatures of x-ray bursts [1]. Reliable predictions on the beyond experimental reach characteristics of these proton-rich nuclei require self-consistent microscopic description of the experimentally accessible properties. Recently we investigated the interplay between isospin-symmetry breaking and shape coexistence effects on the structure of $A = 70$ and $A = 74$ analogs within the *complex* excited Vampir variational model [2]. In the present work we extended our investigations to the β-decay properties of the $Z = N + 2$ members of these isovector triplets in the frame of the *complex* excited Vampir model using the same effective interaction and model space. Our aim is to realistically describe the strength distributions and half-life for ^{70}Kr and ^{74}Sr weak decay under terrestrial conditions and to present predictions on their characteristic behavior in the x-ray burst astrophysical environment. The present study is the first attempt at a completely self-consistent calculation of the terrestrial and stellar weak interaction rates for ^{70}Kr and ^{74}Sr at densities $\rho = 10^4$–10^7 g/cm^3 and temperatures $T = 10^8$–10^{10} K using the *complex* excited Vampir approach.

Investigations based on the variational approaches of the Vampir model family have been successfully performed for coexistence phenomena manifested by proton-rich nuclei in the $A \sim 70$ mass region, in particular, on exotic structure as well as allowed Fermi (F) and Gamow-Teller (GT) β-decay properties of nuclei close to the $N = Z$ line [2–9]. The *complex* excited Vampir approach allows for a unified description of

structure and dynamics at low and high spins including in the symmetry projected mean fields neutron-proton correlations in both $T = 1$ and $T = 0$ channels and general two-nucleon unnatural-parity correlations. The beyond-mean-field *complex* excited Vampir model allows to realistically describe the characteristic features of nuclei in the $A \sim 70$ mass region like shape coexistence and mixing and the strong variation of the deformation with number of nucleons, increasing spin, and excitation energy. The Vampir results nicely compare to the available experimental information and many predictions are confirmed by the data. Since the Vampir approaches enable the use of rather large model spaces and of general two-body interactions, *large-scale* nuclear structure studies going far beyond the abilities of the conventional shell-model configuration-mixing approach are possible. Previous investigations on coexistence phenomena in $N \simeq Z$ nuclei in this mass region indicated for a given symmetry the presence of a variable sometimes strong mixing of differently deformed configurations in the intrinsic system. Furthermore, as expected, besides the like-nucleon pairing, the neutron-proton pairing correlations were found to play an important role ([2] and references therein).

We shall briefly describe the *complex* excited Vampir variational procedure and define the effective Hamiltonian in the next section. Then in Sec. III we shall discuss the results on the β-decay strength distributions and half-life of ^{70}Kr and ^{74}Sr under terrestrial conditions and in the astrophysical x-ray burst environment.

II. THEORETICAL FRAMEWORK

The *complex* excited Vampir (EXVAM) approach uses the most general Hartree-Fock-Bogoliubov (HFB) vacua as basic building blocks being only restricted by time-reversal and axial symmetry. The underlying HFB transformations are essentially *complex* and do mix proton with neutron states as well as states of different parity and angular momentum. The HFB vacua of this type account for arbitrary two-nucleon correlations and thus simultaneously describe like-nucleon as well as isovector and isoscalar neutron-proton pairing correlations. The broken symmetries of these vacua (nucleon numbers, parity, total angular momentum) are restored by projection before variation and the resulting symmetry-projected configurations are then used as test wave functions. Chains of successive

_____
[*]spetro@nipne.ro

variational calculations are accomplished independently in the even-even parent and odd-odd daughter nucleus for each spin and parity to determine the underlying HFB transformations. First the Vampir solutions, representing the optimal mean-field description of the yrast states by single symmetry-projected HFB determinants are obtained. Then the excited Vampir approach is used to construct additional excited states by independent variational calculations. The final solutions for each considered symmetry are obtained diagonalizing the residual interaction between the successively constructed orthogonal many-nucleon excited Vampir configurations.

For nuclei in the $A \sim 70$ mass region we use a ^{40}Ca core and include the $1p_{1/2}$, $1p_{3/2}$, $0f_{5/2}$, $0f_{7/2}$, $1d_{5/2}$, and $0g_{9/2}$ oscillator orbits for both protons and neutrons in the valence space. We start with an isospin symmetric basis and then introduce the Coulomb shifts for the proton single-particle levels resulting from the ^{40}Ca core by performing spherically symmetric Hartree-Fock calculations using the Gogny-interaction D1S in a 21 major-shell basis [5]. The effective two-body interaction is constructed from a nuclear matter G matrix based on the charge-dependent Bonn one-boson-exchange potential Bonn CD. In order to enhance the pairing correlations this G matrix was modified by adding short-range (0.707 fm) Gaussians with strength of -35 MeV in the $T = 1$ proton-proton and neutron-neutron channel, -20 MeV in the neutron-proton $T = 1$ channel, and -35 MeV in the neutron-proton $T = 0$ channel. In addition, the isoscalar interaction was modified by monopole shifts for all $T = 0$ matrix elements of the form $\langle 1p1d_{5/2}; IT = 0|\hat{G}|1p1d_{5/2}; IT = 0\rangle$, where $1p$ denotes either the $1p_{1/2}$ or the $1p_{3/2}$ orbit, and $\langle 0g_{9/2}0f; IT = 0|\hat{G}|0g_{9/2}0f; IT = 0\rangle$, where $0f$ denotes either the $0f_{5/2}$ or the $0f_{7/2}$ orbitals [2]. These monopole shifts have been introduced in our earlier calculations in order to influence the onset of deformation. Previous results indicated that the oblate-prolate coexistence and mixing at low spins sensitively depend on the strengths of the neutron-proton $T = 0$ matrix elements involving nucleons occupying the $0f_{5/2}$ or $0f_{7/2}$ and $0g_{9/2}$ single particle orbits. The Hamiltonian includes the two-body matrix elements of the Coulomb interaction between the valence protons.

III. RESULTS AND DISCUSSION

For the investigation of the Fermi and Gamow-Teller β-decay properties of the lowest two 0^+ and 2^+ states in ^{70}Kr and ^{74}Sr we extended the calculations presented in [2] to the daughter states in the ^{70}Br and ^{74}Rb nuclei, respectively. We constructed up to 80 many-nucleon *complex* excited Vampir configurations for the spin 1^+ and 3^+ in ^{70}Br and ^{74}Rb. The structure of the even-spin yrast states in both parent ^{70}Kr and ^{74}Sr and daughter nuclei ^{70}Br and ^{74}Rb, respectively, was already discussed [2]. In ^{70}Kr the wave functions of the ground state and yrast 2^+ state are dominated by prolate components (almost 73%), the first excited 0^+ indicates almost equal prolate (48%) and oblate (52%) content, while second 2^+ state is dominated by oblate configurations in the intrinsic system (almost 73%). In ^{74}Sr the wave functions of the ground state and yrast 2^+ state are also dominated by prolate components (73% and 88%, respectively), but the first
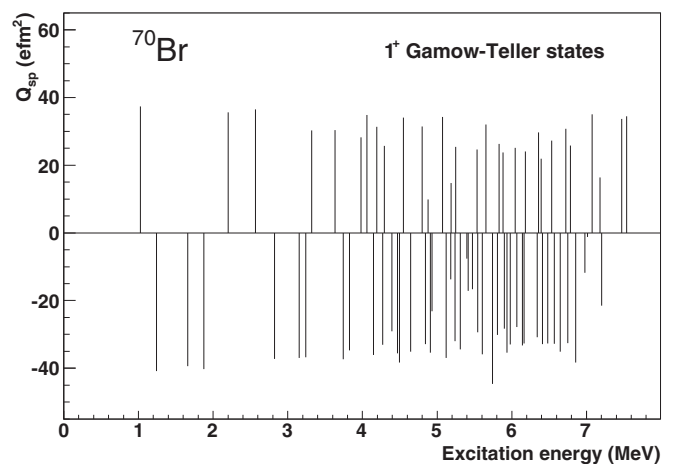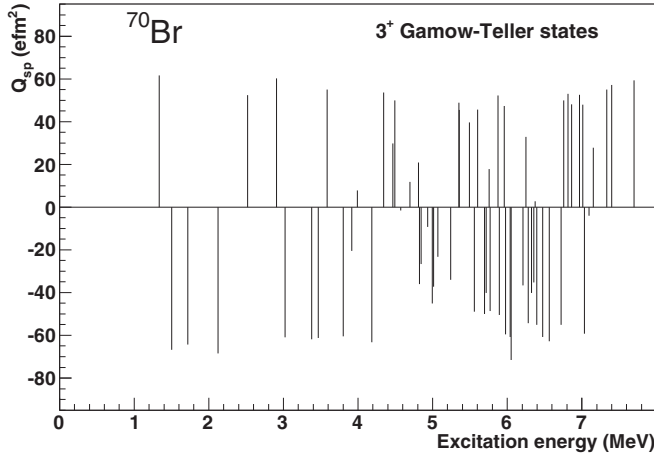

FIG. 1. Spectroscopic quadrupole moments for daughter 1^+ states in ^{70}Br.
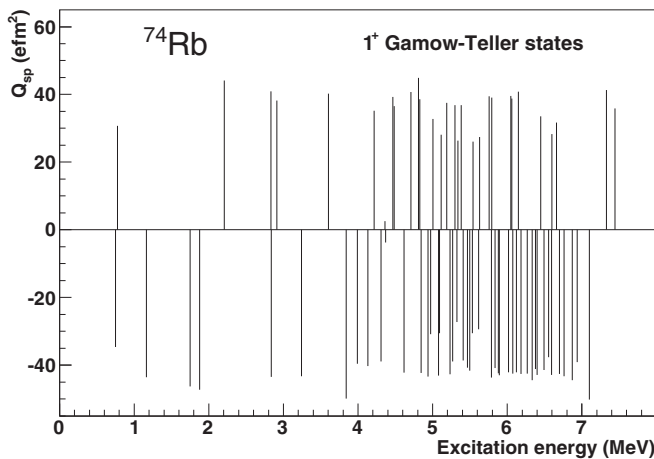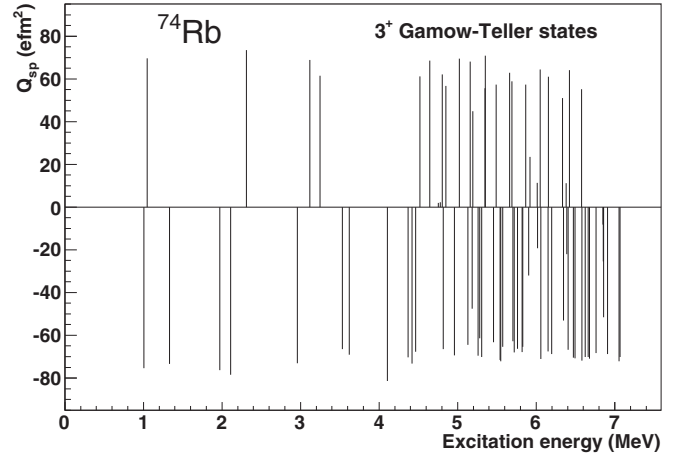
excited 0^+ and the second 2^+ are both dominated by oblate components (68% and 89%, respectively). Strong, similar oblate-prolate mixing was found in the lowest 0^+ and 2^+ states in ^{70}Br, for both spins obtaining almost 70% prolate (oblate) content in the lowest (first excited) state. In ^{74}Rb the mixing is smaller for both lowest two states 0^+ and 2^+, the lowest state indicating almost 86% (95%) prolate content for 0^+ (2^+), while for the first excited state 84% oblate content for 0^+ and 95% for 2^+. Significant difference is found in the energy interval between the lowest two 0^+ and 2^+ states in ^{70}Kr and ^{74}Sr. In ^{70}Kr the lowest two 0^+ (2^+) states are separated by 1.718 (0.982) MeV, while in ^{74}Sr this interval amounts to 0.564 (0.352) MeV. Consequently, in the astrophysical scenarios on the effective half-life in the x-ray burst environment we considered only the contributions from the ground state and the yrast 2^+ state in ^{70}Kr, but from the lowest two 0^+ and 2^+ states in ^{74}Sr. As we may expect a variable, for some states a very strong mixing of differently deformed prolate and oblate configurations in the intrinsic system was found in the structure of the wave functions for the daughter 1^+ and 3^+ states in ^{70}Br and ^{74}Rb. Since we constructed only up to 80 1^+ and 3^+ states in the odd-odd daughter nuclei we may expect that the higher-lying configurations not included in the *complex* excited Vampir many-nucleon bases could introduce more correlations in the structure of the lowest calculated states. Consequently, we assumed for the excitation energy of the lowest 3^+ state the experimental available value, $E_{3^+}(^{70}\text{Br}) = 1.336$ MeV and $E_{3^+}(^{74}\text{Rb}) = 1.006$ MeV, and for the other 3^+ and 1^+ states the relative values with respect to the lowest 3^+ state. The large variety of shape mixing in the structure of the states populated by Gamow-Teller β decay of ^{70}Kr and ^{74}Sr is reflected by the spectroscopic quadrupole moments of the corresponding states in Figs. 1–4.

The *complex* excited Vampir results on the Gamow-Teller strength distributions for the lowest two 0^+ states in ^{70}Kr indicate different behavior reflecting the difference in the mixing of the lowest two main configurations of opposite sign of the quadrupole deformation building the wave functions of the parent 0^+ states. It is worthwhile to mention that the

FIG. 2. The same as in Fig. 1, but for 3^+ states.

FIG. 4. The same as in Fig. 3, but for 3^+ states.

strongest branches in the decay of the ground state are feeding 1^+ states in the daughter nucleus showing spectroscopic quadrupole moments of different sign (the second and the fifth 1^+ with increasing excitation energy). The analysis of the structure of the GT branches to the lowest five 1^+ states indicates that strong branches are built out either from a coherent contribution of $p_{1/2}^{\nu(\pi)} p_{3/2}^{\pi(\nu)}$, $p_{3/2}^{\nu} p_{3/2}^{\pi}$, $f_{5/2}^{\nu} f_{5/2}^{\pi}$, $f_{5/2}^{\nu(\pi)} f_{7/2}^{\pi(\nu)}$, and $g_{9/2}^{\nu} g_{9/2}^{\pi}$ matrix elements or from a strong contribution of $g_{9/2}^{\nu} g_{9/2}^{\pi}$ ones, while weak GT branches show cancellation of all these contributing matrix elements. The analysis of the GT strength distributions for the decay of the yrast 2^+ in ^{70}Kr to 1^+ states in ^{70}Br indicates similar behavior with the GT decay of the ground state, but much weaker branches, while stronger branches are revealed by the strength distribution to the 3^+ states. Very weak transition strengths have been found for the decay of the yrast 2^+ state in ^{70}Kr to 2^+ states in ^{70}Br.

The GT accumulated strengths presented in Fig. 5 for the decay of the ground state, first excited 0^+, and yrast 2^+ state in ^{70}Kr to the daughter states in ^{70}Br indicate stronger strength from the ground state decay with respect to that from the first excited 0^+ state and larger contributions from the decay of the

yrast 2^+ state to the daughter 3^+ states than the ones to the 1^+ states.

In order to evaluate the half-life under terrestrial conditions as well as in the x-ray burst environment we calculated the effect of the isospin mixing on the superallowed Fermi β decay of the ground state and yrast 2^+ state in ^{70}Kr to the analog states in ^{70}Br. Our results indicate for the decay of ^{70}Kr a depletion of the ground to ground transition of 1.95% with the missing strength distributed over many excited 0^+ states. The strongest nonanalog branches are feeding the fourth and the fifth 0^+ states in ^{70}Br situated around 3 MeV excitation energy with un upper limit of 0.4% of the total strength. For the decay of the yrast 2^+ state in ^{70}Kr the depletion of the analog branch amounts to 2.98% and a significant nonanalog branch is feeding the fourth 2^+ state in ^{70}Br with an upper limit of 1.3% of the total strength.

We calculated the half-life of ^{70}Kr using β window $Q_{EC} = 10.480$ MeV [10,11]. The terrestrial half-life for the decay of
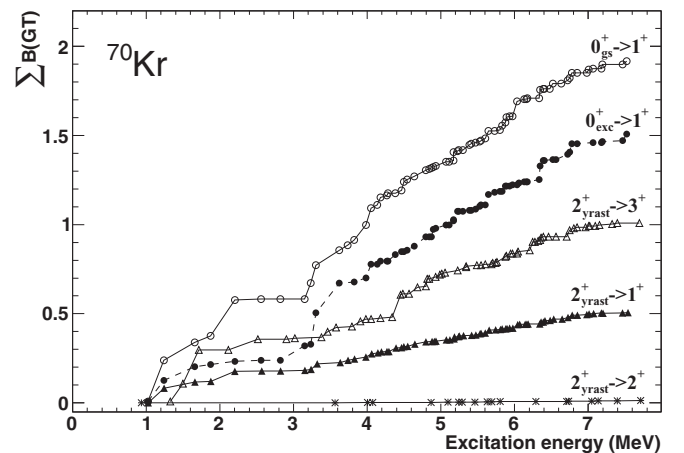

FIG. 3. The same as in Fig. 1, but for ^{74}Rb.

FIG. 5. Gamow-Teller accumulated strengths [in units of $(g_A/g_V)^2$] for the decay of the ground state, first excited 0^+, and yrast 2^+ state in ^{70}Kr to the daughter states in ^{70}Br obtained within the *complex* excited Vampir model.

the ground state of ^{70}Kr is given by

$$\frac{1}{T_{1/2}} = \frac{1}{K} \sum_{E_f} f(Z, E_f)[B_{if}(F) + B_{if}(\text{GT})], \qquad (1)$$

where E_f denotes the energy of the final state, $K = 6146$ s and the Fermi integrals $f(Z, E_f)$ are taken from Ref. [12]. The Fermi and Gamow-Teller reduced transition probabilities can be written as

$$B_{if}(F) = \frac{1}{2J_i + 1}|M_F|^2, \qquad (2)$$

$$B_{if}(\text{GT}) = \frac{1}{2J_i + 1}\left(\frac{g_A}{g_V}\right)^2|M_{\text{GT}}|^2, \qquad (3)$$

where $g_A/g_V = -1.26$. The Fermi and Gamow-Teller nuclear matrix elements between the initial ($|\xi_i J_i >$) and the final ($|\xi_f J_f >$) states of spin J_i and J_f, respectively,

$$M_F \equiv (\xi_f J_f||\hat{1}||\xi_i J_i)$$
$$= \delta_{J_i J_f} \sum_{ab} M_F(ab)(\xi_f J_f||[c_a^\dagger \tilde{c}_b]_0||\xi_i J_i), \qquad (4)$$

$$M_{\text{GT}} \equiv (\xi_f J_f||\hat{\sigma}||\xi_i J_i)$$
$$= \sum_{ab} M_{\text{GT}}(ab)(\xi_f J_f||[c_a^\dagger \tilde{c}_b]_1||\xi_i J_i), \qquad (5)$$

are composed of the reduced single-particle matrix elements of the unit operator 1, $M_F(ab) = (a||\hat{1}||b)$, and Pauli spin operator σ, $M_{\text{GT}}(ab) = 1/\sqrt{3}(a||\hat{\sigma}||b)$, and the reduced one-body transition densities calculated using the harmonic oscillator wave functions [13]. For β^+-decay and electron capture, $c_a^\dagger$ is the neutron creation operator and $\tilde{c}_b$ is the proton annihilation operator and the sum runs over the valence nucleons. The *complex* excited Vampir result for the Gamow-Teller half-life of the ground state of ^{70}Kr is 258 ms and for the Fermi decay is 63 ms. Consequently, the theoretical half-life of the ground state amounts to 51 ms in good agreement with the available experimental values of 57(21) ms [14], 42(31) ms [15], adopted 52(17) ms [16], and the most recent preliminary value of 40(6) ms [17]. The comparison of our predictions to the experimental data from high-resolution measurements with the EURICA device obtained at RIKEN on the Gamow-Teller strength distribution is expected in the near future. For a possible comparison with total absorption spectrometer results we folded the GT strength distribution with a Gaussian function of 60 keV width, but the result on the half-life is not changed, while using an width of 1 MeV a reduction of about 16% is obtained. Previously published QRPA calculations failed to account for the half-life of ^{70}Kr [18], but more recent results suggest fairly well description [19].

For ^{74}Sr we calculated the Gamow-Teller strength distributions for the decay of the lowest two 0^+ and 2^+ states to the daughter 1^+, 2^+, and 3^+ states in ^{74}Rb. The strengths of the branches feeding the low-lying 1^+ states indicate completely different behavior for ground state and first excited 0^+ state decay and opposite to the situation found in ^{70}Kr the weaker contributions originate from the decay of the ground state.

The strength distributions for the decay of the lowest two 2^+ states in ^{74}Sr to 1^+ states in ^{74}Rb manifest different behavior
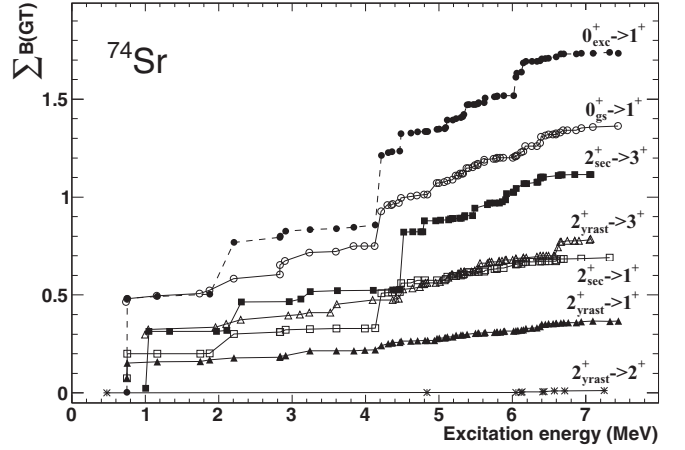

FIG. 6. Gamow-Teller accumulated strengths [in units of $(g_A/g_V)^2$] for the decay of the ground state, first excited 0^+, yrast, and second 2^+ states in ^{74}Sr to the daughter states in ^{74}Rb obtained within *complex* excited Vampir model.

with increasing energy. Also the distributions displayed by the yrast and second 2^+ state indicate completely different evolution at low energies compared to the ground state and first excited 0^+ state decay, respectively, but again the strongest branches are decaying the second 2^+ state. The strength distributions for the decay of the lowest two 2^+ states to the 3^+ states in ^{74}Rb manifest different behavior. The decay of the second 2^+ state indicates similarities with corresponding decay to the 1^+ states. Very weak strengths are obtained for the decay of both 2^+ states to daughter 2^+ states in ^{74}Rb. The Gamow-Teller accumulated strengths are presented in Fig. 6. Opposite to the trend obtained for ^{70}Kr, in the ^{74}Sr decay the GT accumulated strength for the decay of the first excited 0^+ state is stronger than the characteristic one for the ground state. Also for the spin 2^+ both types of contributions, to the 1^+ and 3^+ states in ^{74}Rb, are stronger for the decay of the second 2^+ state. The analysis of the structure of the GT branches for the decay of the ground state to the lowest two 1^+ states manifesting very strong and very weak strengths, respectively, indicates that the first one is built out of a coherent contribution of $p_{1/2}^{\nu(\pi)} p_{3/2}^{\pi(\nu)}$, $p_{3/2}^{\nu} p_{3/2}^{\pi}$, $f_{5/2}^{\nu} f_{5/2}^{\pi}$, $f_{5/2}^{\nu(\pi)} f_{7/2}^{\pi(\nu)}$, and $g_{9/2}^{\nu} g_{9/2}^{\pi}$ matrix elements, while the weak GT branch shows a cancellation of all these contributing matrix elements.

The calculated depletion due to the isospin mixing for the superallowed Fermi β decay of the ground state and yrast 2^+ state in ^{74}Sr to the analog states in ^{74}Rb amounts to 3% and 3.6%, respectively. The missing strength in the decay of the ground state is distributed over many 0^+ states in ^{74}Rb with un upper limit for the branch to the second and the sixth excited 0^+ state of 0.8% from the total strength. In the decay of the yrast 2^+ state in ^{74}Sr two significant nonanalog branches feed the second (1.3%) and the fourth (0.8%) 2^+ states in ^{74}Rb and the rest of the strength is distributed over many 2^+ states.

We calculated the half-life of ^{74}Sr under terrestrial conditions using β window $Q_{EC} = 11.090$ MeV [11,20]. The *complex* excited Vampir result for the Gamow-Teller decay half-life of the ground state of ^{74}Sr is 137 ms and for the Fermi decay is 48 ms. Consequently, the theoretical half-life of the

ground state of ^{74}Sr amounts to 36 ms in good agreement with the available experimental value of 27(8) ms [21,22]. Results on the half-life based on QRPA calculations assuming an oblate shape for the ground state of ^{74}Sr indicate 54 ms for $Q_{EC} = 11.2$ MeV [19] and 27 ms for $Q_{EC} = 12.2$ MeV [21].

The agreement between the *complex* excited Vampir results for the terrestrial decay and the available data on half-lives gives support to our predictions on the β-decay strength distributions for the low-lying excited states in ^{70}Kr and ^{74}Sr isotopes. Using the present predictions as well as our previous results [2] concerning the excitation energy of these states we shall present in the following the *complex* excited Vampir results on the stellar weak interaction rates for these nuclei in the x-ray burst environment. The general formalism to calculate weak interaction rates for a stellar environment has been introduced by Fuller *et al.* [23]. Relevant for the astrophysical scenarios of explosive phenomena are the properties of exotic nuclei difficult to investigate experimentally or beyond the experimental reach [24–26]. Previous studies suggested that in the ranges of densities and temperatures relevant for the rp process the stellar β decay and continuum electron capture characteristics are sensitive to the strength distributions. Consequently, a realistic description of the shape coexistence and mixing dominating the structure of the low-lying states of $A \sim 70$ proton-rich nuclei and the corresponding daughter states is required. The rate for the weak processes is given by

$$\lambda^{\alpha} = \frac{\ln 2}{K} \sum_i \frac{(2J_i + 1)e^{-E_i/(kT)}}{G(Z,A,T)} \sum_j B_{ij} \phi_{ij}^{\alpha}, \quad (6)$$

where α stays for the considered processes (β^+ decay and continuum electron capture), the constant $K = 6146$ s, the sums in i and j run over the thermally populated parent states i of spin J_i and excitation energy E_i and j daughter states, respectively. G is the partition function of the parent nucleus (Z,A) defined by $G(Z,A,T) = \sum_i (2J_i + 1) \exp{(-E_i/(kT))}$. B_{ij} contains the allowed Fermi and Gamow-Teller transition probabilities,

$$B_{ij} = B_{ij}(F) + B_{ij}(GT). \quad (7)$$

The last factor ϕ_{ij}^{α} is the phase space integral for the two calculated processes, β^+ decay and continuum electron capture, given by

$$\phi_{ij}^{\beta^+} = \int_1^{Q_{ij}} wp(Q_{ij} - w)^2 F(-Z + 1, w)$$
$$\times (1 - S_p(w))(1 - S_\nu(Q_{ij} - w))dw, \quad (8)$$

$$\phi_{ij}^{ec} = \int_{w_l}^{\infty} wp(Q_{ij} + w)^2 F(Z,w)S_e(w)(1 - S_\nu(Q_{ij} + w))dw, \quad (9)$$

where w is the total, rest mass and kinetic, energy of the electron or positron in units of $m_e c^2$, $p = \sqrt{w^2 - 1}$ is the momentum in units of $m_e c$, and Q_{ij} is the total energy available in β^+ decay in units of $m_e c^2$,

$$Q_{ij} = \frac{1}{m_e c^2}(M_p - M_d + E_i - E_j), \quad (10)$$

where M_p, M_d are the nuclear masses of the parent and daughter nucleus, respectively, whereas E_i, E_j are the excitation energies of the initial and final states. Depending on Q_{ij} the threshold is $w_l = 1$ if $Q_{ij} > -1$, or $w_l = |Q_{ij}|$ if $Q_{ij} < -1$. The Fermi function, $F(Z,w)$ [12], correcting the phase space integral for the Coulomb distortion of the electron or positron wave function near the nucleus is approximated by

$$F(Z,w) = 2(1 + \gamma)(2pR)^{-2(1-\gamma)} \frac{|\Gamma(\gamma + iy)|^2}{|\Gamma(2\gamma + 1)|^2} e^{\pi y}, \quad (11)$$

where $\gamma = \sqrt{1 - (\alpha Z)^2}$, $y = \alpha Z w/p$, α is the fine structure constant, and R is the nuclear radius. S_e, S_p, and S_ν are the electron, positron, and neutrino distribution functions, respectively. In the rp process astrophysical environment electrons and positrons are well described by Fermi-Dirac distributions, with temperature T and chemical potential μ by

$$S_e = \frac{1}{\exp[(E_e - \mu_e)/(kT)] + 1} \quad (12)$$

with $E_e = wm_e c^2$. The positron distribution is defined similarly with $\mu_p = -\mu_e$. The chemical potential, μ_e, is determined from the density ρ (in g/cm^3) inverting the relation

$$\rho Y_e = \frac{1}{\pi^2 N_A}\left(\frac{m_e c}{\hbar}\right)^3 \int_o^{\infty}(S_e - S_p)p^2 dp \quad (13)$$

(in mol/cm^3), where Y_e is the electron-to-baryon ration (in mol/g), and N_A is Avogadro's number. The density of electron-positron pairs has been removed by forming the difference $S_e - S_p$. In the rp-process scenarios it is assumed that $S_\nu = 0$ and $S_p = 0$ [24].
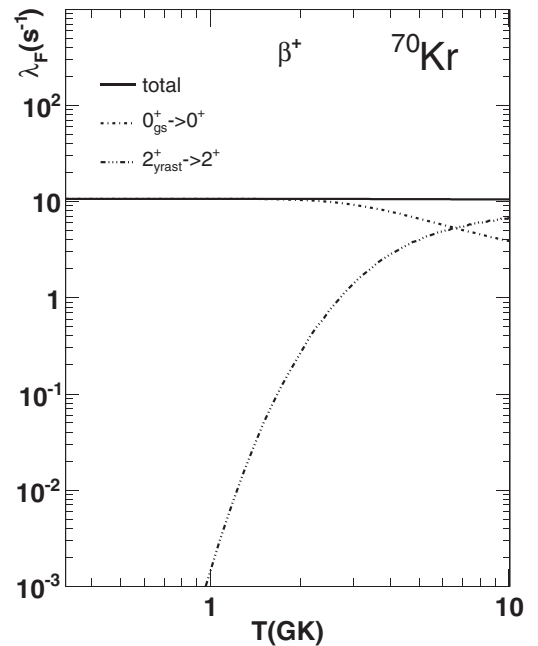

FIG. 7. Fermi β-decay rates (s^{-1}) for the ground state and yrast 2^+ state of ^{70}Kr as a function of temperature T (GK) obtained within *complex* excited Vampir model.

FIG. 8. Gamow-Teller β-decay rates (s^{-1}) for the ground state and yrast 2^+ state of ^{70}Kr as a function of temperature T (GK) obtained within *complex* excited Vampir model.
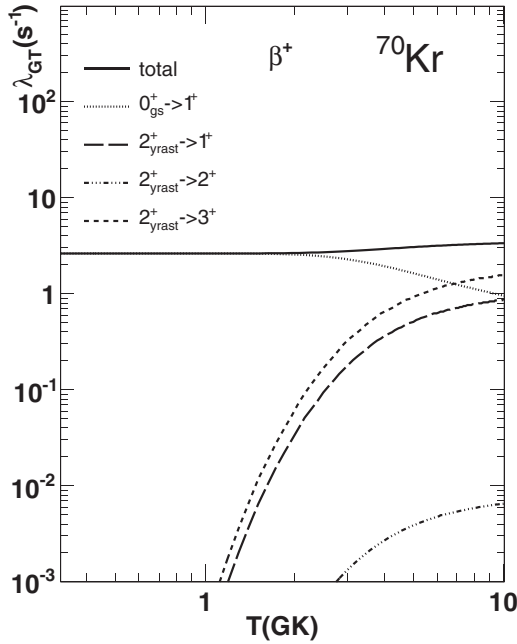

FIG. 10. Fermi and Gamow-Teller decay rates (s^{-1}) for the ground state and yrast 2^+ state of ^{70}Kr decomposed into the corresponding β^+ and electron capture components for selected densities ρY_e (mol/cm^3) (left) and total decay rates for rp-process peak density (right) as a function of temperature T (GK).

For the $Z = N + 2$ nucleus ^{70}Kr we investigated the influence of the yrast 2^+ state decay on the effective half-life given the predicted high excitation energy of the first excited 0^+ and the second 2^+ states. In Fig. 7 the Fermi β-decay rates for the ground state and yrast 2^+ state of ^{70}Kr as a function of temperature are presented. The Gamow-Teller β-decay rates as a function of temperature decomposed into contributions from the ground state of ^{70}Kr to the daughter 1^+ states in ^{70}Br and from yrast 2^+ state to the daughter 1^+, 2^+, and 3^+ are depicted in Fig. 8. The influence of the decay of the 2^+ state on the total decay rate appears only at temperatures $T > 2.5$ GK. In Fig. 9 the Fermi and Gamow-Teller β-decay and continuum electron capture rates for rp-process peak density $\rho Y_e = 10^6$ (mol/cm^3) are decomposed into the contributions from the

ground state and yrast 2^+ state of ^{70}Kr to the daughter states in ^{70}Br. As it is illustrated in Fig. 10 (left) the contribution of the electron capture is very small at the temperatures (1–3 GK) and densities (10^6–10^7 g/cm^3) characteristic for the rp-process astrophysical environment. Our previous investigations on the stellar weak interaction rates for the waiting point nuclei ^{68}Se and ^{72}Kr revealed a very strong contribution from the continuum electron capture at the rp-process peak conditions [27]. The total decay rates for ^{70}Kr at the rp-process peak density as a function of temperature are presented in Fig. 10 (right) decomposed into the contributions from the ground state and yrast 2^+ state.
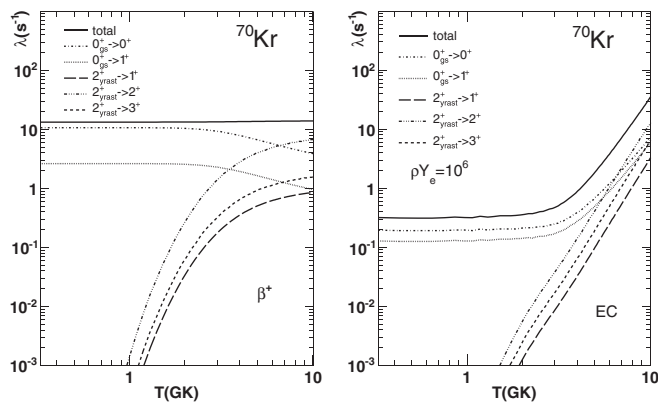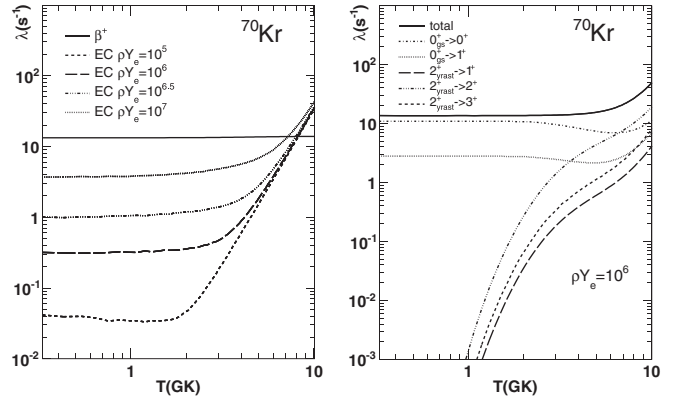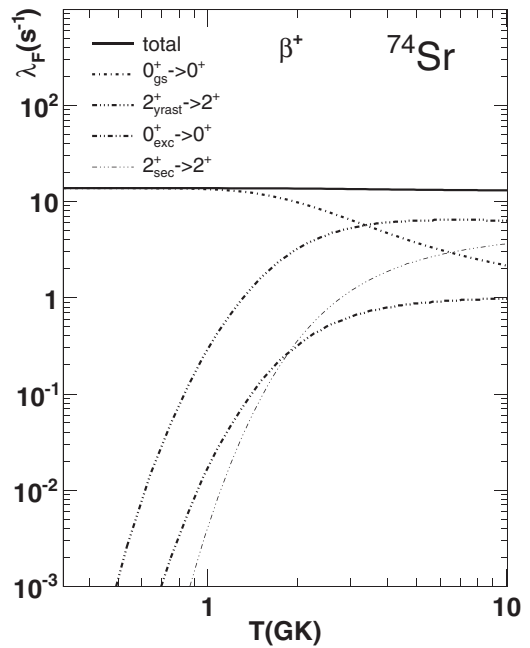

FIG. 9. Fermi and Gamow-Teller decay rates (s^{-1}) of ^{70}Kr for β^+ (left) and continuum electron capture for rp-process peak density ρY_e (mol/cm^3) (right) as a function of temperature T (GK).

FIG. 11. Fermi β-decay rates (s^{-1}) for the ground state, first excited 0^+, yrast, and second 2^+ state of ^{74}Sr as a function of temperature T (GK).
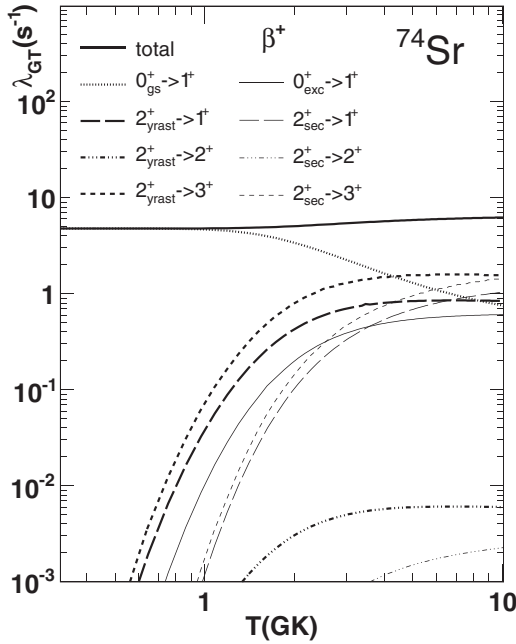
FIG. 12. Gamow-Teller β-decay rates (s^{-1}) for the ground state, first excited 0^+, yrast, and second 2^+ state of ^{74}Sr as a function of temperature T (GK).

FIG. 14. Continuum electron capture decay rates (s^{-1}) for the lowest two 0^+ and 2^+ states of ^{74}Sr at rp-process peak density as a function of temperature T (GK).

For the $Z = N + 2$ nucleus ^{74}Sr we studied the influence of the decay of the thermally populated first excited 0^+, yrast, and second 2^+ state on the stellar half-life as a function of temperature and densities. In Fig. 11 the Fermi β-decay rates for the lowest two 0^+ and 2^+ parent states to the daughter states in ^{74}Rb as a function of temperature are illustrated.

The Gamow-Teller β-decay rates as a function of temperature presented in Fig. 12 are decomposed into contributions from all four considered states in ^{74}Sr to the corresponding daughter states.

Increase in the GT total decay rates produced by the low-lying excited parent states could be seen for temperatures $T >$ 2 GK. The Fermi and Gamow-Teller β^+-decay rates presented in Fig. 13 as a function of temperature are decomposed in contributions from the parent states in ^{74}Sr to the daughter states in ^{74}Rb. Continuum electron capture rates decomposed into the corresponding contributions are illustrated in Fig. 14
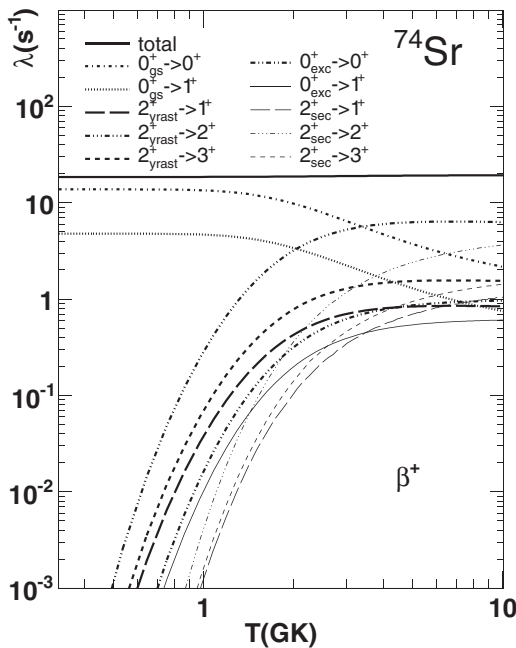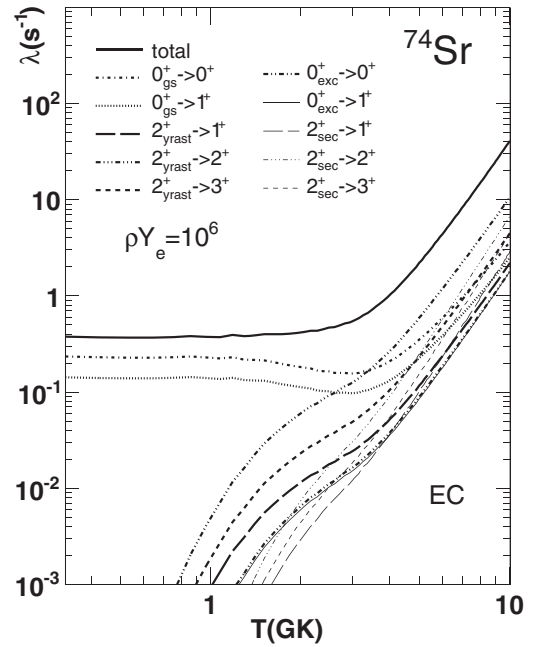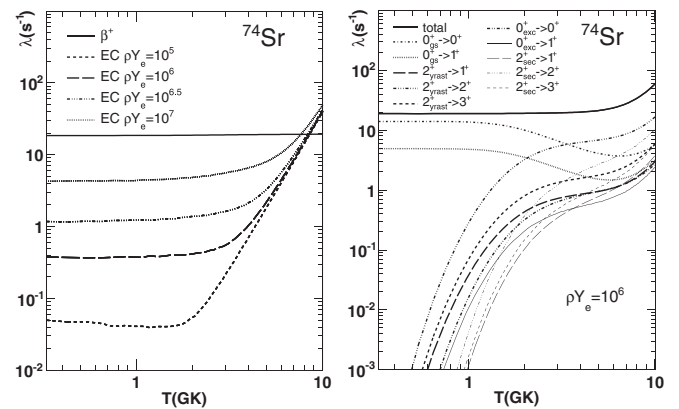

FIG. 13. Fermi and Gamow-Teller β-decay rates (s^{-1}) for the ground state, first excited 0^+, yrast, and second 2^+ state of ^{74}Sr as a function of temperature T (GK).

FIG. 15. Fermi and Gamow-Teller decay rates (s^{-1}) for the lowest two 0^+ and 2^+ states of ^{74}Sr decomposed into β^+ and electron capture components for selected densities ρY_e (mol/cm^3) (left) and total decay rates for rp-process peak density (right) as a function of temperature T (GK).
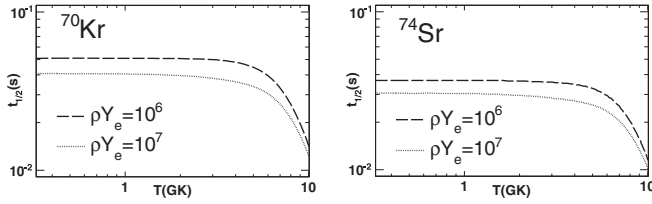
FIG. 16. Half-lives (s) for ^{70}Kr (left) and ^{74}Sr (right) for selected densities ρY_e (mol/cm^3) as a function of temperature T (GK).

as a function of temperature at rp-process peak density $\rho Y_e = 10^6$ (mol/cm^3). In ^{74}Sr, like in ^{70}Kr decay, the continuum electron capture contribution is very small with respect to the β^+ contribution in the range of temperature and density specific for the rp-process conditions as it is illustrated in Fig. 15 (left). Total decay rates at rp-process peak density decomposed into the contributions from different parent states are presented in Fig. 15 (right) as a function of temperature. Finally, in Fig. 16 are presented the half-lives for ^{70}Kr and ^{74}Sr for two selected densities ρY_e as a function of temperature. The results indicates that under rp-process typical conditions the effective half-lives are not changed with respect to the values found under terrestrial conditions. At peak density $\rho Y_e = 10^6$ (mol/cm^3) and $T = 2$ GK the calculated half-life for ^{70}Kr is 51 ms and for ^{74}Sr is 36 ms. As can be inferred from Fig. 16 these values almost do not vary under rp-process conditions, $\rho Y_e = 10^6$ (mol/cm^3) and $T = 1$–3 GK [1] (numerical information is available in [28]). Similar trend was observed in QRPA calculations taking into account only the decay of the ground state [19].

The present report represent the first beyond-mean-field treatment based on an effective two-body interaction constructed from the nuclear matter G matrix starting from the charge dependent Bonn CD potential able to describe self-consistently the allowed Fermi and Gamow-Teller β decay as well as the effect of the isospin mixing on the structure of the corresponding isovector triplets [2] in a region dominated by shape coexistence and mixing. Furthermore, we use a model space adequate for the description of proton-rich nuclei in the $A \sim 70$ mass region which is not yet numerically feasible for the large-scale shell-model calculations. In a previous report [27] a comparison of the *complex* excited Vampir results obtained in the model space usually involved in our studies on nuclei in the $A \sim 70$ mass region (the one used in the present work) and a larger model space including besides the $d_{5/2}$ and $g_{9/2}$, the $d_{3/2}$ and $g_{7/2}$ spherical orbitals for both protons and neutrons is presented. The conclusion is that similar results are obtained for the same effective interaction in the two model spaces for terrestrial as well as stellar investigated properties. Experimental strength distributions and spectroscopic quadrupole moments for the parent and daughter states could test our predictions on the influence of shape mixing on weak interaction rates.

IV. CONCLUSIONS

In this article we present the first self-consistent results on the effect of shape mixing on the weak interaction rates for the $Z = N + 2$ isotopes ^{70}Kr and ^{74}Sr describing the low-lying 0^+ and 2^+ states in the parent nuclei and the corresponding daughter 0^+, 1^+, 2^+, and 3^+ states in ^{70}Br and ^{74}Rb, respectively, within the *complex* excited Vampir model based on the effective interaction obtained from the charge-dependent Bonn CD potential and the adequate model space previously used to investigate the effect of the isospin mixing in the isovector triplets with $A = 70$ and $A = 74$. Of course, experimental information is needed on the strength distributions for the ^{70}Kr and ^{74}Sr decay to confirm our predictions. The application of our results to the stellar weak interaction rates started with the investigation of the ^{68}Se and ^{72}Kr rp-process waiting points [27] and is currently extended to $N = Z$ nuclei up to ^{100}Sn.

[1] H. Schatz *et al.*, Phys. Rep. **294**, 167 (1998).

[2] A. Petrovici, Phys. Rev. C **91**, 014302 (2015).

[3] C. Chandler *et al.*, Phys. Rev. C **56**, R2924(R) (1997).

[4] A. Petrovici, K. W. Schmid, and A. Faessler, Nucl. Phys. A **728**, 396 (2003).

[5] A. Petrovici, K. W. Schmid, O. Radu, and A. Faessler, Nucl. Phys. A **747**, 44 (2005).

[6] A. Petrovici, K. W. Schmid, O. Radu, and A. Faessler, Phys. Rev. C **78**, 044315 (2008).

[7] A. Petrovici, K. W. Schmid, O. Andrei, and A. Faessler, Phys. Rev. C **80**, 044319 (2009).

[8] A. Petrovici, J. Phys. G: Nucl. Part. Phys. **37**, 064036 (2010).

[9] A. Petrovici, K. W. Schmid, and A. Faessler, Progr. Part. Nucl. Phys. **66**, 287 (2011).

[10] J. Savory *et al.*, Phys. Rev. Lett. **102**, 132501 (2009).

[11] M. Wang, G. Audi, A. H. Wapstra, F. G. Kondev, M. Mac-Cormick, X. Xu, and B. Pfeiffer, Chin. Phys. C **36**, 1603 (2012).

[12] N. B. Gove and M. J. Martin, Nucl. Data Tables **10**, 205 (1971).

[13] K. W. Schmid, F. Grümmer, and A. Faessler, Ann. Phys. (NY) **180**, 1 (1987).

[14] M. Oinonen *et al.*, Phys. Rev. C **61**, 035801 (2000).

[15] B. Blank, Eur. Phys. J. A **15**, 121 (2002).

[16] J. K. Tuli, Nucl. Data Sheets **103**, 389 (2004).

[17] A. M. Rogers, Nucl. Data Sheets **120**, 41 (2014).

[18] P. Sarriguren, E. Moya de Guerra, and A. Escuderos, Phys. Rev. C **64**, 064306 (2001).

[19] P. Sarriguren, Phys. Rev. C **83**, 025801 (2011).

[20] S. Ettenauer *et al.*, Phys. Rev. Lett. **107**, 272501 (2011).

[21] J. Henderson *et al.*, Phys. Rev. C **90**, 051303(R) (2014).

[22] B. Singh, ENSDF www.nndc.bnl.gov (2015).

[23] G. M. Fuller, W. A. Fowller, and M. J. Newman, Astrophys. J. Suppl. Ser. **42**, 447 (1980); Astrophys. J. **252**, 715 (1982); Astrophys. J. Suppl. Ser. **48**, 279 (1982); Astrophys. J. **293**, 1 (1985).

[24] K. Langanke and G. Martinez-Pinedo, Rev. Mod. Phys. **75**, 819 (2003).

[25] J. Pruet and G. M. Fuller, Astrophys. J. Suppl. Ser. **149**, 189 (2003).

[26] S. E. Woosley *et al.*, Astrophys. J. Suppl. Ser. **151**, 75 (2004).

[27] A. Petrovici and O. Andrei, Eur. Phys. J. A **51**, 133 (2015).

[28] http://niham.nipne.ro/stellar.pdf.